Assignement 4 - Shallow water and Roe scheme

SF2521

Non-horizontal bottom - High resolution scheme

Authors :
Valentin Duvivier
Damien Lussan

Under the guidance of :
Patrick Henning
Johan Wärnegård

April 14th 2020

Contents

1 Introduction

This report synthesizes the work done for the home assignment n°4. This report will mainly consist in working on the wave equation using the Roe flux and to then extend it for higher resolution scheme.

First, we will introduce the idea of a non-horizontal bottom in the case of shallow water.

Then, we will develop the Roe scheme and compare it with Lax-Friedrich scheme from HW2.

To finish, we will extend this scheme for higher resolution.

We will finally conclude on the Roe scheme regarding the results obtained throughout this report.

2 Shallow water model - non-horizontal bottom

In this section, we will be considering the following system of equation :

$$\begin{pmatrix} h_t \\ hu_t \end{pmatrix} + \begin{pmatrix} h_x u + h u_x \\ h u u_x + g h (h_x + B_x) \end{pmatrix} = \begin{pmatrix} 0 \\ 0 \end{pmatrix} \tag{1}$$

2.1 Still water

We consider the above system considering no speed (u = 0) as we consider a still water. We are now willing to see the repercussions on this system :

$$\begin{pmatrix} h_t \\ h \times 0 \end{pmatrix} + \begin{pmatrix} h_x \times 0 + h \times 0 \\ h \times 0 + g h (h_x + B_x) \end{pmatrix} = \begin{pmatrix} 0 \\ 0 \end{pmatrix}$$

$\rightarrow$	$h_t = 0$	$g h (h_x + B_x) = 0$
$\Rightarrow$	h = constant over time	$h + B$ = constant over the mesh

From these equalities here, we know that the wave's height is gonna be constant throughout time when we don't consider speed (speed null).

Furthermore, the sum $h + B$ is gonna be constant over the mesh. This implies that the level of water will be at a defined fix position.

To conclude, **B** being a **constant**, **h** being **independent of time**, and the sum **h**+**B** being **constant** over the **mesh**, we finally know that the water will remain at a fix height and so that the condition of no speed implies a *"horizontal water level"*.

2.2 Re-writing in conservation form

We want to re-write the above system in function of h and m, considering $m = hu$:

$$\begin{pmatrix} h \\ m \end{pmatrix}_t + \begin{pmatrix} m \\ f_2(h,m) \end{pmatrix} = \begin{pmatrix} 0 \\ s(h,m,x) \end{pmatrix}$$

To do so, we will considering each line separately. Moreover, we will use the first line and then implement in on the second one. Indeed, by noting that $m = hu$ we have $m_t = uh_t + u_t h$ and thus $hu_t = m_t - uh_t$.

Thereby :

$$\begin{aligned} & h_t + h_x u + h u_x && = 0 \\ \rightarrow \quad & (hu)_x && = -h_t \\ \Rightarrow \quad & h u_t && = m_t + u(hu)_x \end{aligned}$$

We now implement this relation on the second line of the system :

$$\begin{aligned} m_t \quad & +u(hu)_x + huu_x && +gh(h_x + B_x) && = 0 \\ m_t \quad & +(hu^2)_x && +g(\frac{h^2}{2})_x + ghB_x && = 0 \\ m_t \quad & +(hu^2)_x && +g(\frac{h^2}{2})_x && = -ghB_x \end{aligned} \tag{2}$$

To finish with this sub part, we will now implement the simplification we made on the initial system :

$$\begin{pmatrix} h \\ m \end{pmatrix}_t + \begin{pmatrix} hu \\ hu^2 + \frac{1}{2}gh^2 \end{pmatrix}_x = \begin{pmatrix} 0 \\ -ghB_x \end{pmatrix}$$

$$\Rightarrow \quad \begin{pmatrix} h \\ m \end{pmatrix}_t + \begin{pmatrix} m \\ \frac{m^2}{h} + \frac{1}{2}gh^2 \end{pmatrix}_x = \begin{pmatrix} 0 \\ -ghB_x \end{pmatrix} \tag{3}$$

By identification, with the general form we have, we conclude on :

- $f_2(h,m) = \frac{m^2}{h} + \frac{1}{2}gh^2$
- $s(h,m,x) = -ghB_x$

NOTE : we did define as expected f_2 as a function of h and m and $s(h,m,x)$ such that this function is independent of the derivatives of h or m.

3 First order Roe scheme

During this part, we will introduce a new flux : the **Roe flux** ; that we will implement into a conservation scheme.

We consider the first order Roe numerical flux that follows :

$$\mathbf{F}^n_{i+1/2} = \frac{1}{2}(\mathbf{f}(\mathbf{Q}^n_i) + \mathbf{f}(\mathbf{Q}^n_{i+1})) - \frac{1}{2}|\tilde{\mathbf{A}}_{i+1/2}|(\mathbf{Q}^n_{i+1} - \mathbf{Q}^n_i)$$

Which is simplified in

$$\mathbf{F}_{i+1/2} = \frac{1}{2}(\mathbf{f}(\mathbf{Q}_i) + \mathbf{f}(\mathbf{Q}_{i+1})) - \frac{1}{2}\sum_{p=1}^{2} |\hat{\lambda}^p_{j+1/2}|\mathbf{W}^p_{j+1/2}$$

An important element on this report is the eigen-values $\hat{\lambda}$. Indeed, as we will consider a flow using the wave equation, each λ will in fact have the physical meaning of a speed, information that will see itself useful.
We then see that to compute this flux numerically, we will have to declare the eigenvalues and eigenvectors :

Eigen-values :

$$\begin{pmatrix} \hat{\lambda}^1 \\ \hat{\lambda}^2 \end{pmatrix} \quad = \quad \begin{pmatrix} \hat{u} - \hat{c} \\ \hat{u} + \hat{c} \end{pmatrix} \quad \equiv \quad \begin{pmatrix} \frac{m}{h} - \sqrt{gh} \\ \frac{m}{h} + \sqrt{gh} \end{pmatrix} \tag{4}$$

Eigen-vectors :

$$\hat{r}^1 = \begin{bmatrix} 1 \\ \lambda^1 \end{bmatrix} \qquad \text{and} \qquad \hat{r}^2 = \begin{bmatrix} 1 \\ \lambda^2 \end{bmatrix} \tag{5}$$

with

$$\begin{aligned} \hat{u} &= \frac{\sqrt{h_j}u_j + \sqrt{h_{j+1}}u_{j+1}}{\sqrt{h_j} + \sqrt{h_{j+1}}} \\ \hat{c} &= \sqrt{g\bar{h}} \\ \bar{h} &= \frac{1}{2}(h_j + h_{j+1}) \end{aligned}$$

To conclude on the scheme used in this assignment, we considered a finite volume in conservation form, based on central difference and forward Euler, applied on ROE's flux :

$$Q^{n+1}_j = Q^n_j - \frac{\Delta_t}{\Delta_x}(\mathbf{F}_{j+1/2}(Q^n_{j+1}, Q^n_j) - \mathbf{F}_{j-1/2}(Q^n_j, Q^n_{j-1})) \tag{6}$$

3.1 Flat bottom

3.1.1 Single pulse

We are willing to find the condition on $m(x,0)$ such that we have initially a single pulse.

We know that the eigenvalues of our system represent the speed of the waves. As we have two eigen-values, we have two waves each one define by its own speed.

We also know that during the HW2 we ran a similar code with $m(x,0) = 0$, and that we then have had two symmetrical waves of same amplitude moving at the same speed. As we want a unique pulse, we see that we need one of our eigenvalue to be null. We then move into a unique direction. Therefore, we have two possibilities for our initial condition :

$$
\begin{array}{lll}
 & \text{If} & \lambda^1 = 0 \\
\rightarrow & & m(x,0) = (h-H)\sqrt{gh} \\
\rightarrow & & \lambda^2 > 0 \\
\Rightarrow & & \text{a pulse moving } \textbf{rightward}
\end{array}
$$

$$
\begin{array}{lll}
 & \text{If} & \lambda^2 = 0 \\
\rightarrow & & m(x,0) = -(h-H)\sqrt{gh} \\
\rightarrow & & \lambda^1 < 0 \\
\Rightarrow & & \text{a pulse moving } \textbf{leftward}
\end{array}
$$

In the followings we will consider a rightward oriented flux and thereby we consider the first of the two above cases : $\lambda^1 = 0 \rightarrow m(x,0) = (h-H)\sqrt{gh}$.

In the following parts, we will study more precisely our scheme considering this unique pulse.

3.1.2 Variation of N_x (mesh's size)

During this part, we considered the following values for our scheme :

- $\mathbf{L = 10}$, length of the mesh [m];
- $N_x = [80, 160, 320]$, number of cell [-] ;
- $\rightarrow \Delta_x = \frac{L}{(N_x - 1)} \approx [\frac{1}{8}, \frac{1}{16}, \frac{1}{32}]$

- $\mathbf{T = 20}$, duration of the study [s] ;
- $N_t = [600, 1220, 2470]$, number of iteration in time [-] ;
- $\rightarrow \Delta_t = \frac{T}{N_t} = [\frac{1}{30}, \frac{1}{61}, \approx \frac{1}{124}]$

NOTE :

- We took N_t such that it is as low as possible, while ensuring stability ;
- We then remark that we get the following CFL condition :

$$\lambda_{CFL} = \frac{\Delta_t}{\Delta_x} \leq \frac{1}{4}$$

We want to study the influence of the mesh's sizing. To do so, we will run our numerical scheme considering the three mesh sizes (N_x) defined above.

We then display the plots for one bounce on the wall at $x = L$:

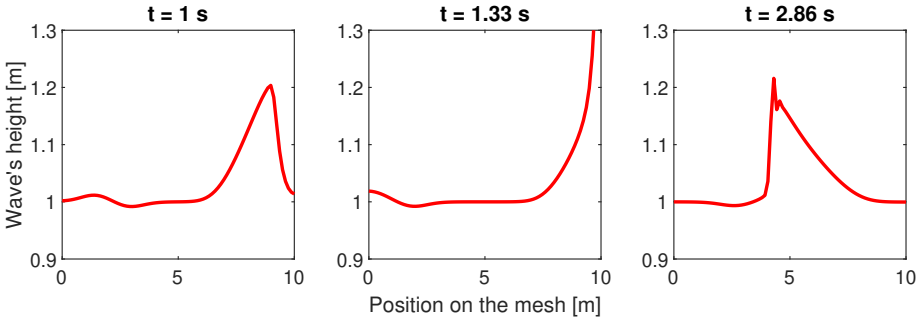

Figure 1: Wave's bouncing at n = 80

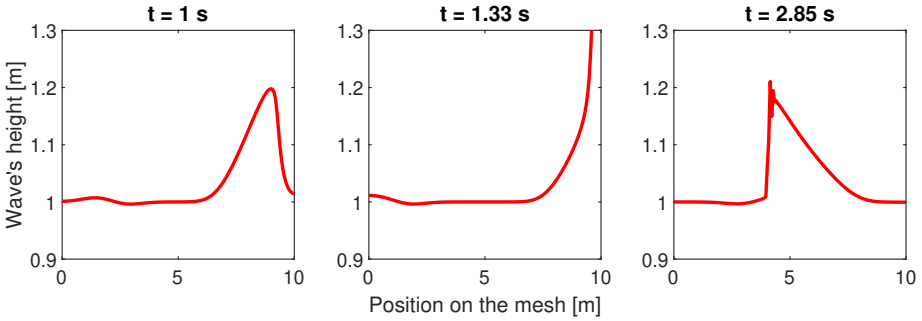

Figure 2: Wave's bouncing at n = 160

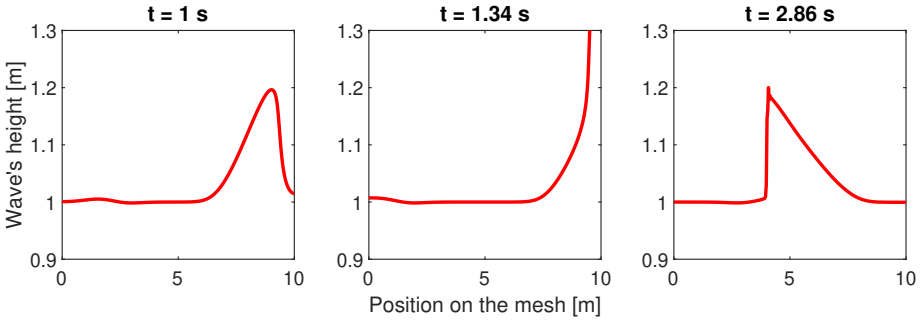

Figure 3: Wave's bouncing at n = 320

On these graphs, we observe an overall similitude. We note anyway that there is some **oscillations** behind the wave and that are visible on the graphs at t = 1s and t = 2s.
These artificial oscillations show the limit of the numerical scheme we are using. By refining it, and so by increasing the number of cells, we see that one reduces these artificial oscillations, that then tend to flatten.

To finish, the shape of the wave after rebound looks sharper. It indeed has the appearance of a smooth initial value developing a **discontinuity**. Nevertheless, as we know the wave will remain stable during this study, we can only conclude that the wave presents a local artificial discontinuity that, together with the artificial oscillations, correspond to the denomination of **dispersion**.

The following part will aim in having a more precise idea in how the function behaves when we don't consider a viscous term. To do so, we will compare the ROE scheme with the Lax-Friedrich one.

3.1.3 Comparison Lax-Friedrich / Roe fluxes

To see how relevant is the flux used during this assignment, we are now aiming in comparing these results with the equivalent obtained from Lax-Friedrich's scheme. We thereby keep the same data than before, keeping a CFL number as big as possible while ensuring stability.

Below, you have graphs superposing the graphs for both methods, considering the different mesh's sizes :

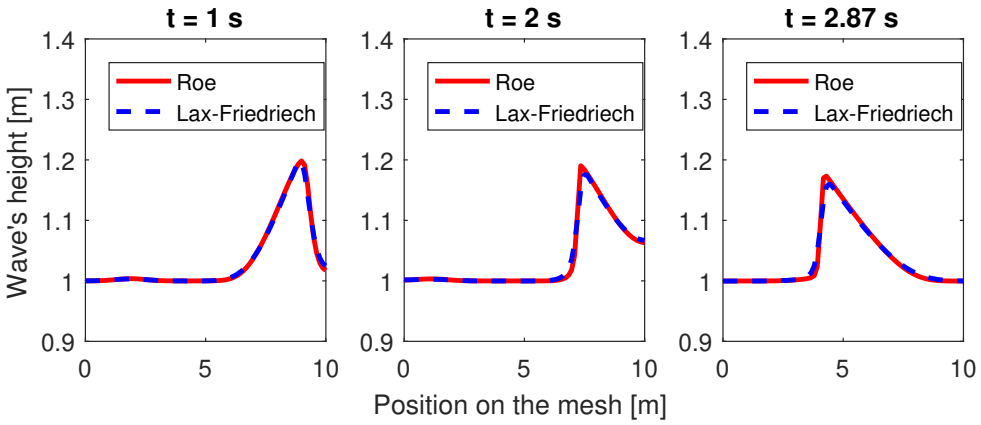

Figure 4: Comparison ROE / Lax Friedrich at n = 80

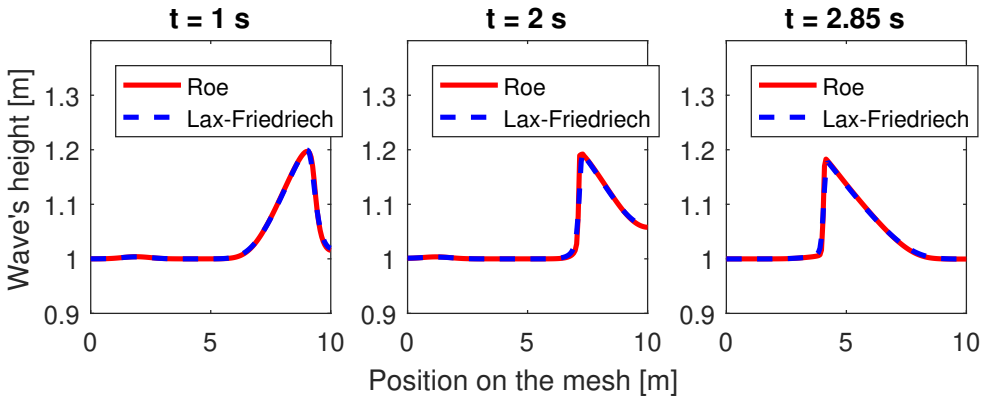

Figure 5: Comparison ROE / Lax Friedrich at n = 160

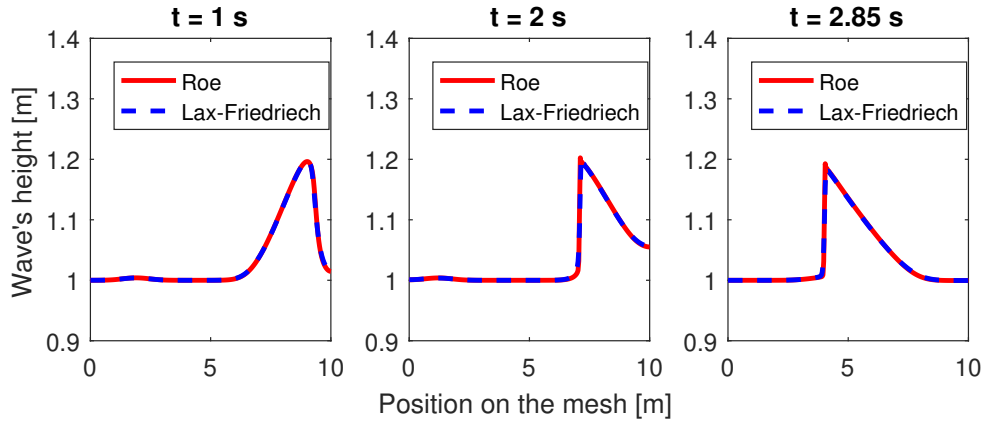

Figure 6: Comparison ROE / Lax Friedrich at n = 320

We first note an overall similitude between the graphs. Nevertheless, by looking more precisely to the first group of graphs, we see that we have dissipation.

For instance, on the third graph at $n = 80$, we see a consequent diminishing of the amplitude and a little stretching of the Lax-Friedrich graph towards the sides.

This observation of the sharps being smoothed and curves, as well as the apparition of a curve kind of "flattening" is then what responds to the denomination **dissipation**.

Once, again, by increasing the number of cell, our graph get even smoother and the two fluxes give similar results.
However, we can take a final look to the two fluxes for a lower CFL number. We will then be able to conclude on the general trending and not only on the particular case close to the discontinuity case.

Here below, we then plotted the comparison considering the same time frame but for $n = 320$ and $\lambda_{CFL} \approx 0.1$ (instead of 0.25) :

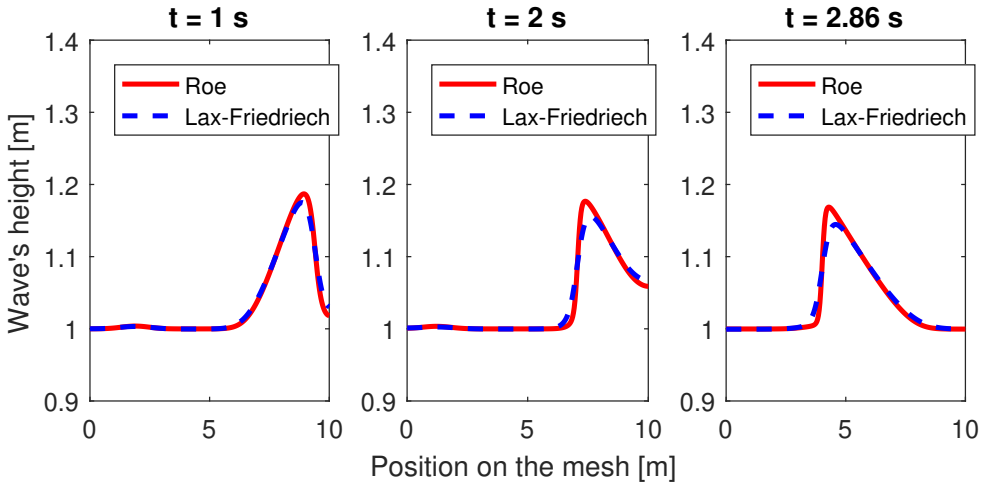

Figure 7: Comparison ROE / Lax Friedrich at n = 320 and $\lambda_{CFL} \approx 0.1$

From this graph, we conclude on the fact that the Lax-Friedrich scheme, which is a **monotone scheme**, presents **bigger dissipation with respect to the Roe scheme**.

To go deeper into how well behaves the ROE scheme, with respect to the Lax-Friedrich one, we will analyse the characteristics discussed above : dissipation, instabilities, etc.

3.1.4 Accuracy, dissipation and dispersion

First, to check the accuracy of the scheme, we look at the order of accuracy of Δ_x and Δ_t :

Δ_x	u_h	$u_h - u_{h/2}$	$(u_h - u_{h/2}/u_{h/2} - u_{h/4})$	$log_2(u_h - u_{h/2}/u_{h/2} - u_{h/4})$
4.3	$-4.6 * 10^{-10}$	$-3.1 * 10^{-8}$	12.3	3.6
8.6	$-4.1 * 10^{-11}$	$-4.1 * 10^{-10}$	3.0	1.6
17.1	$-6.5 * 10^{-12}$	$-3.4 * 10^{-11}$	1.96	0.97
34.2	$4.9 * 10^{-12}$	$-1.1 * 10^{-11}$	1.94	0.95
68.5	$1.1 * 10^{-11}$	$-1.7 * 10^{-11}$		
137	$1.4 * 10^{-11}$			

Table 1: Order of accuracy on Δ_x

Δ_t	u_h	$u_h - u_{h/2}$	$(u_h - u_{h/2}/u_{h/2} - u_{h/4})$	$log_2(u_h - u_{h/2}/u_{h/2} - u_{h/4})$
$1.2 * 10^{-4}$	$-1.8 * 10^{-8}$	$-1.4 * 10^{-9}$	4.9	2.3
$5.9 * 10^{-4}$	$-3.7 * 10^{-10}$	$-1.7 * 10^{-9}$	3.0	1.6
$3.0 * 10^{-5}$	$-7.7 * 10^{-11}$	$-10 * 10^{-11}$	2.3	1.2
$1.5 * 10^{-5}$	$2.3 * 10^{-11}$	$-4.2 * 10^{-11}$	2.2	1.1
$7.3 * 10^{-6}$	$6.5 * 10^{-11}$	$-1.9 * 10^{-11}$		
$3.7 * 10^{-6}$	$8.4 * 10^{-11}$			

Table 2: Order of accuracy on Δ_t

We conclude regarding the values obtained that both Δ_x and Δ_t are of **order 1**.

For what is up to the dissipation and the dispersion :

- The **dispersion** on one hand, is a phenomenon appearing clearly when we have a high CFL number. Then, artificial discontinuities make their appearance on the top of the wave as well as at its back.
  This phenomenon shows that to study complex flow, we have to use schemes presenting some virtual discontinuities.
  Finally, the dispersion for both schemes tend to disappear when we refine the mesh.

- The dissipation on the other hand is observable in any conditions, even though it is visually more perceptible at a CFL number different from the limit one.
  This phenomenon results into a flow flattened and stretched, having the behavior of a local diffusion.
  Regarding our graphs, it appears clear that the Lax-Friedrich scheme presents more dissipation with respect to the Roe one.

- We conclude on the fact that the Lax-Friedrich scheme appears as a smoothed approximation of the flow we model, while the ROE scheme sticks more to the reality but also presents some virtual discontinuities

3.1.5 Case $a = 2 * H$

To finish with the study of the Roe flux on a flat bottom, we take a look back to our initial condition m(x,0). In fact, instead of $a = \frac{H}{5}$ we compute our scheme for $a = 2 \times H$. To do so had led us into modifying the time step in order to ensure the stability.
However, to make a consistent comparison we decided to consider again a number of iteration such that we were at the limit CFL number.
Below, we displayed a comparison between the initial case ($a = H/5$) and the current case ($a = 2 \times H$) considering 320 cells :

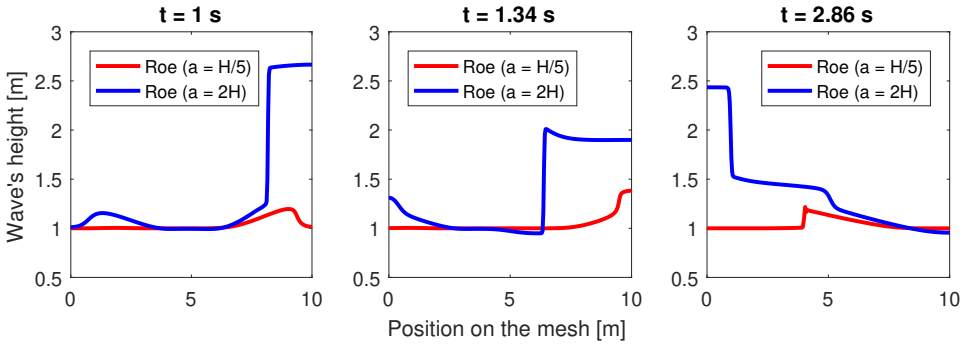

Figure 8: Comparison cases $a = 2 \times H$ and $a = H/5$ for $x = 320$

From these graphs we can conclude on the scheme stability, over the initial condition. Indeed, while we had an expression similar to a linearized formula in a first time, we have here a perturbation parameter that appears to be bigger than the constant term coming with it.

Thus, as our function isn't oscillating anymore around a constant value, we have a non-linear behavior appearing. We then have discontinuities such that the transition between two neighbor cells results in a jump.

We thereby have here a visual idea on why it is important to consider a smooth initial value for the scheme to be stable.

This observation made, we will now head towards an other aspect of the wave equation : studying chocked flow.

3.2 Non-horizontal bottom

We now consider a bump on the bottom defined by :

$$B(x) = \begin{cases} B_0 cos^2(\frac{\pi(x-L/2)}{2r}) & |x - L/2| < r \\ 0 & |x - L/2| \geq r \end{cases}$$

that we introduce on the ROE scheme as follows :

$$Q_j^{n+1} = Q_j^n - \frac{\Delta_t}{\Delta_x}(F_{j+1/2}^n - F_{j-1/2}^n) + \Delta_t S(Q^n) \tag{7}$$

with $F_{j\pm1/2}^n$ the numerical flux functions for S = 0.

In this part we will study the effect of an uneven bottom on the flow's regime. We will therefore study the cases of super and sub critical flow.

3.2.1 Boundary condition

First, we have to define new boundary condition to make the super and sub critical flow possible.

We want to use as well extrapolation BC and Dirichlet conditions on m(x) and/or h(x). While the first one implies to fix ourselves the value at the boundary, the extrapolation implies to define the cell at the edge in function to the ones at proximity.

These two cases lead to the following boundary conditions :

- **Sub-critical** : $\lambda^1 < 0$ and $\lambda^2 > 0$. We then have two opposed waves and we thereby have to fix conditions on each boundary. We here put Dirichlet BC on the two edges' neighbors : **m fixed** at $\mathbf{x = 0}$ and **h fixed** at $\mathbf{x = L}$; and we have extrapolation condition for the two other parameters.

- **Super-critical** : $\lambda^{1,2} > 0$. We then have the two waves going into the same direction, and so we only fix the conditions at one of the two edges. We here put **Dirichlet BC** at $\mathbf{x = 0}$ for **m and h** ; while we used extrapolation condition at x = L.

NOTE : these inequalities for the eigen-values stand under the assumption of a right headed wave.

In our case, we used this formula below for the extrapolation :

- $k(0,t) = 2 * k(1,t) - k(2,t) \quad$ and $\quad k(N+2,t) = 2 * k(N+1,t) - k(N,t)$, with k = h,m ;

The table below summarizes the type of BC we have :

	$h_{\text{left}} = h(0,t)$	$h_{\text{right}} = h(n+1,t)$	$m_{\text{left}} = m(0,t)$	$m_{\text{right}} = m(n+1,t)$
Sub-critical	Extrapolation	Dirichlet condition	Dirichlet condition	Extrapolation
Super-critical	Dirichlet condition	Extrapolation	Dirichlet condition	Extrapolation

Table 3: Boundary conditions for $h(x)$ and $m(x)$

Now that we know what condition to put at the boundaries, we will see the value to consider depending on the flow regime.

3.2.2 Smooth steady state solutions

We will in this part compute steady solutions considering above BC and steady IC. As said in the above part, we consider extrapolation for the outflow and we define the Dirichlet conditions at the inflow (we fix the value at the ghost cell).

Some elements of the following, such that the graphs' shape in detail or the BC, are based on informations that you can find on [1] [2].

- First, we want to compute an "all sub-critical" flow. The conditions we took, with the values, are the following one :

h(x,0)	m(x,0)	h(0,t)	h(n+1,t)	m(0,t)	m(n+1,t)
0.9	1	2*h(1,t) - h(2,t)	0.9	1	2*m(n,t) - m(n-1,t)

Table 4: Sub-critical flow conditions

By running the code, we get the following graph :

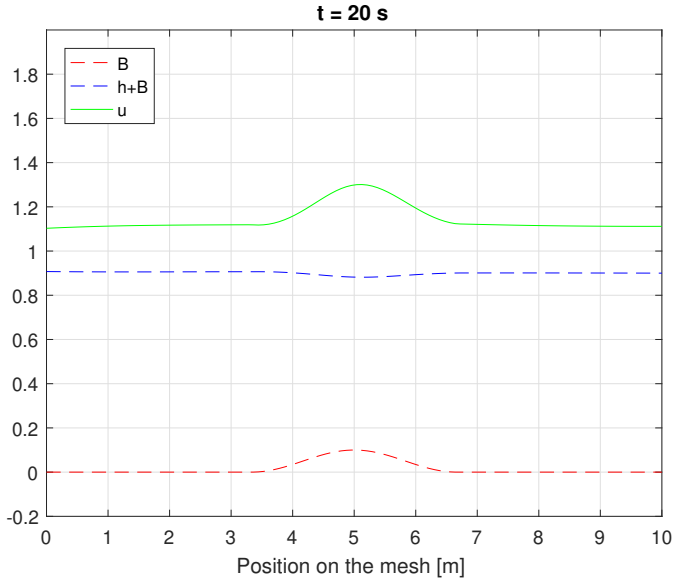

Figure 9: All sub-critical flow

We do have as expected a flow whose speed increases at the bump before decreasing. We thereby remain under sub-critical flow conditions. Indeed, with the considered values, the threshold to reach critical flow is $u = \sqrt{gh} \approx 2.97 m.s^{-1}$ which lower from the speed on the graph.

- On the other hand we want to compute an "all super-critical" flow. The conditions we took, with the values, are the following one :

h(x,0)	m(x,0)	h(0,t)	h(n+1,t)	m(0,t)	m(n+1,t)
0.8	3.9	0.8	2*h(n,t) - h(n-1,t)	3.9	2*m(n,t) - m(n-1,t)

Table 5: Sub-critical flow conditions

By running the code, we get the following graph :

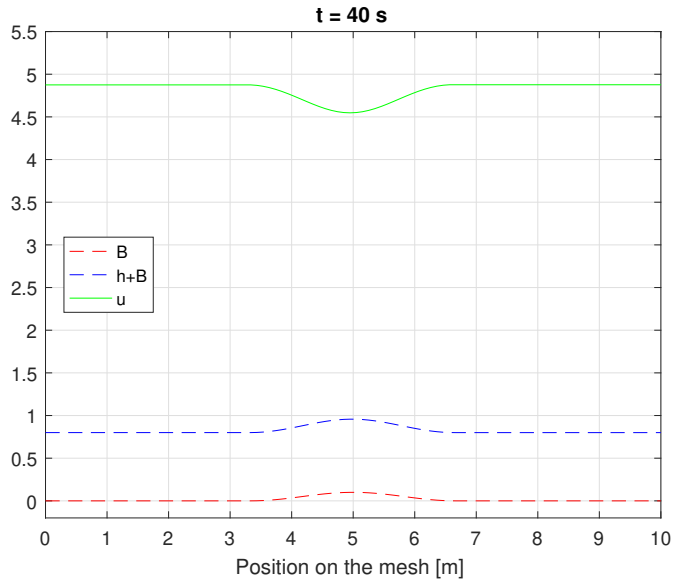

Figure 10: All super-critical flow

Here too we get the expected graph. We then have an all super-critical flow whose speed decelerates at the bump before increasing afterward. We remain at super-critical flow as we have a critical speed equal to $u = 2.80m.s^{-1}$, which is lower than the speed from the graph.

3.2.3 Entropy fix - transonic rarefaction

We now want to observe flows that are, in the same graph, sub- and super- critical. To do so, one must include a term called entropy fix, defined as follows :

$$\Phi_\delta(\lambda) = \begin{cases} |\lambda| & if \ \ |\lambda| \geq \delta \\ \frac{(\lambda^2+\delta^2)}{2\delta} & if \ \ |\lambda| < \delta \end{cases}$$

This function, as you may notice, will smooth the curve by refining the values taken by the scheme where the lower eigen-value get very close to zero. We thereby introduce the threshold δ defining where we refine the mesh.

Anyway, before using this new term, we are first willing to get the curves without adding this entropy fix term to show why it is important to add one.

As we are considering a flow in part sub- and super- critical, the BC will be a combination of the previous one (steady case) :

- When we have a sub-critical flow, we have Dirichlet boundary conditions for the height at $x = L$ and for the moment at $x = 0$; and similarly for the extrapolation conditions ;

- When we have a super-critical flow, we have 2 Dirichlet boundary conditions at $x = 0$, 2 extrapolation conditions at $x = L$.

- We conclude on the fact that wee must have 1 extrapolation condition for the moment at $x = L$, and Dirichlet conditions elsewhere.

What else is gonna change are the values taken by these BC.

- In one hand, we ran the type 3 without entropy fix term. The values of initial and boundary conditions are the following one :

h(x,0)	m(x,0)	h(0,t)	h(n+1,t)	m(0,t)	m(n+1,t)
1	2.1	1	1	2.1	2*m(n,t) - m(n-1,t)

Table 6: Sub-critical flow conditions

and the associated graph is :

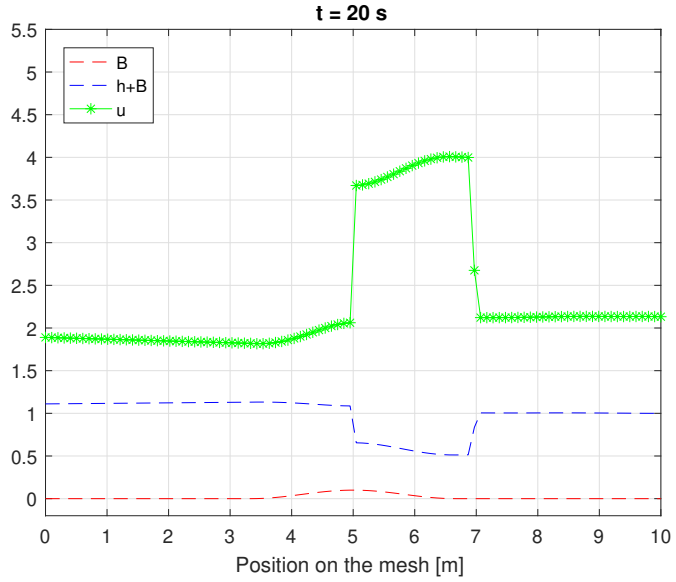

Figure 11: Type 3 graph without entropy fix term

We can see that contrary to what was expected, this graph is coarse. Besides, the transition between sub- and super- critical isn't smooth, on the contrary it makes appear virtual discontinuities at $x = 5$ and $x = 7$.

- On the other hand, we plotted the type 4 graph, still without entropy fix term, using the following BC values :
and here is the associated graph :

Here too, we note a coarse scheme, showing that the transition at x = 5 isn't smooth as one could have expected. Therefore, it will be necessary to apply a method that will result in smoothing this part of the graph.

h(x,0)	m(x,0)	h(0,t)	h(n+1,t)	m(0,t)	m(n+1,t)
1.5	5.5	1.5	1.5	5.5	2*m(n,t) - m(n-1,t)

Table 7: Sub-critical flow conditions

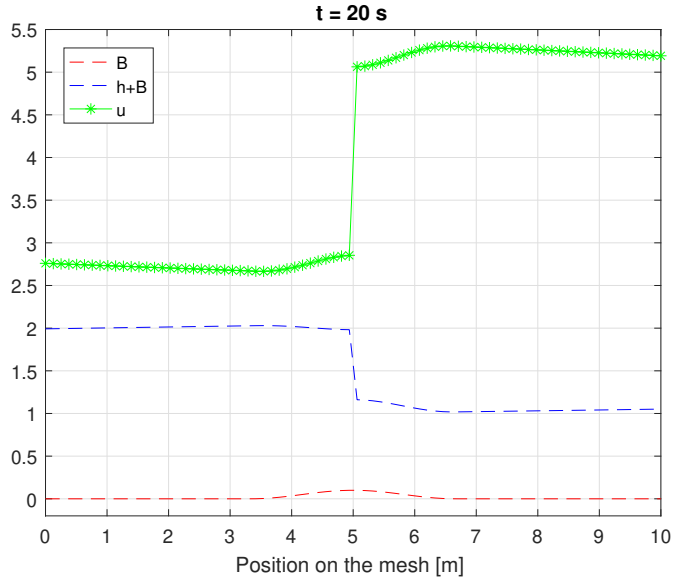

Figure 12: Type 4 graph without entropy fix term

As mentioned before, this method is made by implementing the Harten's entropy fix. On the two following graphs you can see the type 3 and type 4 graphs in the case of the Harten's entropy fix :

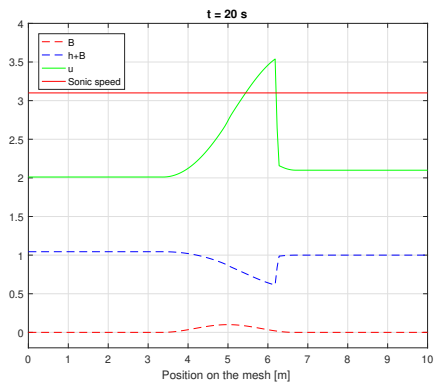

(a) Type 3 graph with entropy fix term

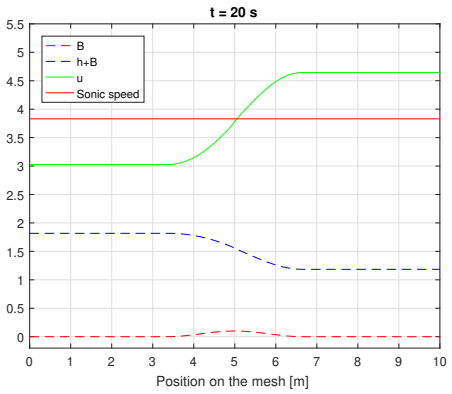

(b) Type 4 graph with entropy fix term

Figure 13: Type 3 and 4 graphs with entropy term

NOTE : the boundary conditions are exactly the same than for the **same cases** with no entropy.

Furthermore, we note a real modification of the graphs that now present a smoother transition between sub- and super-critical cases.

Indeed, with the red line being the threshold for sonic speed, we see that the flow is continuous.

Besides, as expected, on type 3 graph, we reach subcritical speed at the bump before getting back to sub-critical regime afterward; and on type 4 we move from sub- to super-critical flow.

Now and as we did in the previous part, by comparing the cases with and without entropy fix term, we are willing to show what are the differences between the above results and the one provided by the Lax-Friedrich scheme.
From what we have observed before, we are expecting the Lax-Friedrich scheme to present dissipation at long time scale with respect to the Roe scheme.

- On one hand we look at the type 3 case considering the same BC and IC as above :

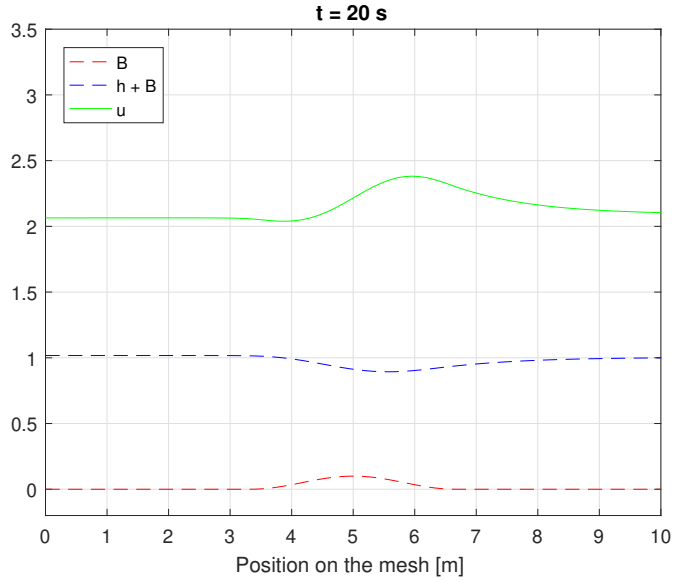

Figure 14: Type 3 graph with Lax-Friedrich scheme

As foretold, **we have** a big **dissipation**. We have the overall same shape that is similar but we have a curve flattened. This observation stands for both the speed and the height.

This information confirms the fact that the Lax-Friedrich scheme is a scheme that comes with dissipation.

- On the other hand we look at the type 4 case considering the same BC and IC as before :

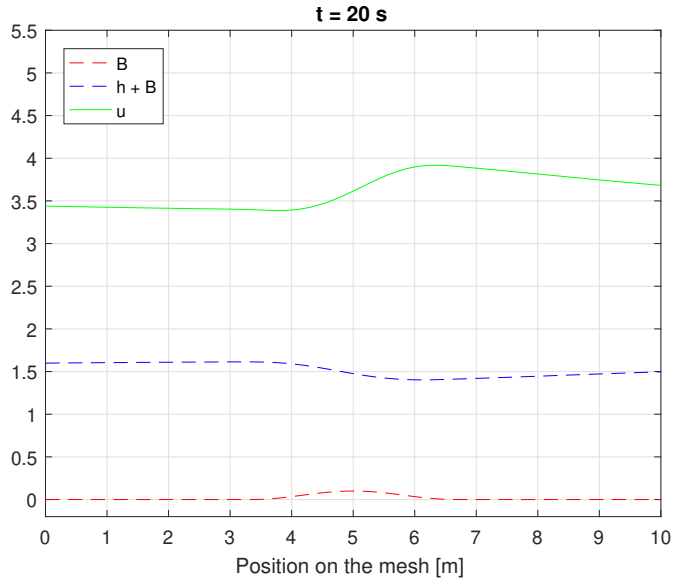

Figure 15: Type 4 graph with Lax-Friedrich scheme

Once again, we see an evident dissipation for the Lax-Friedrich scheme. We remark than even if this graph doesn't strictly stick to the reference one, when we look to the figure 13, we observe the same shape (more precisely at the boundaries). This comfort us into concluding that the scheme is indeed the one we were aiming for and thus that the Lax-Friedrich is dissipative.

To finish with this part, we then can ask ourselves how the entropy function behaves depending on δ.

In the following, we are to see the impact of δ on the curve's continuity.

Thereby, we have below two graphs for type 3 and 4 comparing the results for several values of δ :

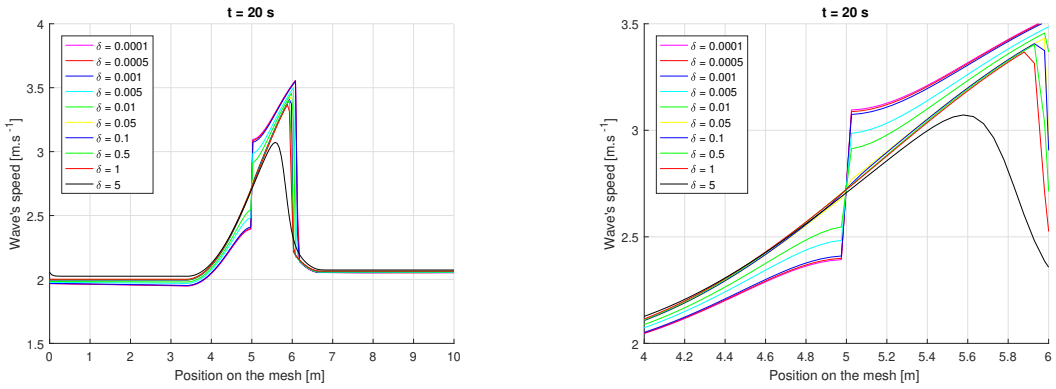

(a) Type 3 for several δ

(b) Zoom on graph

Figure 16: Type 3 depending on δ

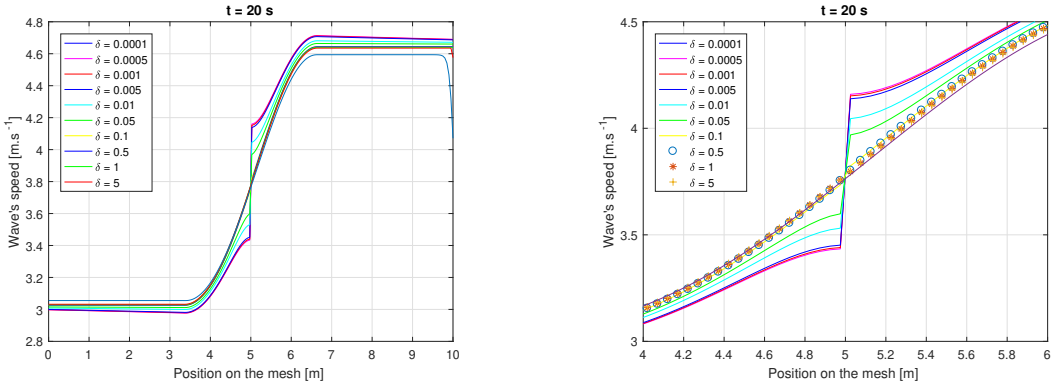

(a) Type 4 for several δ

(b) Zoom on graph

Figure 17: Type 4 depending on δ

Rather than the value taken by δ, what is important to see here is that by decreasing δ, we increase the transition's discontinuity. Moreover, this confirm the idea of a threshold we talked about before : if we reduce the threshold, we smooth less point on the curve, while when we increase it, we are almost always on the smooth case ($|\lambda| < \delta$).

We can conclude on the fact that this **entropy fix term** is able to make the **curve smoother**, adding terms at the **transition** range. The **continuity** is ensured and we therefore **stick to the physical behavior** of the flow.

4 High-resolution Roe scheme

In this part the flux is replaced by $F^n_{i+1/2} + \frac{\Delta t}{\Delta x}\tilde{F}^n_{i+1/2}$:

The flux $\tilde{F}_{i+1/2}$ is given by the equation (15.63) in Leveque:

$$\tilde{F}_{i+1/2} = \frac{1}{2}\sum_{p=1}^{2}\left|s^p_{i+1/2}\right|\left(1 - \frac{\Delta t}{\Delta x}\left|s^p_{i+1/2}\right|\right)\tilde{\mathcal{W}}^p_{i+1/2} \tag{8}$$

Where $s^p = \frac{1}{2}(\lambda^p_{\text{left}} + \lambda^p_{\text{right}})$.

And as said in the subject of the homework, $\tilde{\mathcal{W}}^p_{i-1/2}$ is a limited $\mathcal{W}^p_{i-1/2}$.

$$\tilde{\mathcal{W}}^p_{i-1/2} = \mathcal{W}^p_{i-1/2} \times \varphi(\theta_i) \tag{9}$$

Where the Roe scheme limiter $\varphi(\theta_j)$ is defined as following:

$$\varphi(\theta_i) = \begin{cases} \max(0, \theta_i) & \text{if } |\theta_i| < 1 \\ 1 & \text{if } |\theta_i| \geq 1 \end{cases}$$

with $\theta_i = \frac{Q^n_i - Q^n_{i-1}}{Q^n_{i+1} - Q^n_i}$

Therefore, the high-resolution Roe scheme is:

$$Q^{n+1}_i = Q^n_i - \frac{\Delta t}{\Delta x}\left(F_{i+1/2} - F_{i-1/2} + \frac{\Delta t}{\Delta x}\left(\tilde{F}_{i+1/2} + \tilde{F}_{i-1/2}\right)\right) \tag{10}$$

4.1 High-resolution tests

4.1.1 Comparison Roe/High-resolution Roe/Lax Friederichs schemes

In this part, we are going to run the flat bottom tests that we have seen in section 3.1. Here, the length between both walls is set at $\mathbf{L = 10}$ m with a space discretization set at $\mathbf{n = 400}$ and the time of study is set to $\mathbf{T = 10}$ s for all three schemes. The number of iteration of the time **Nt** is set to either **5000** or **8000**.

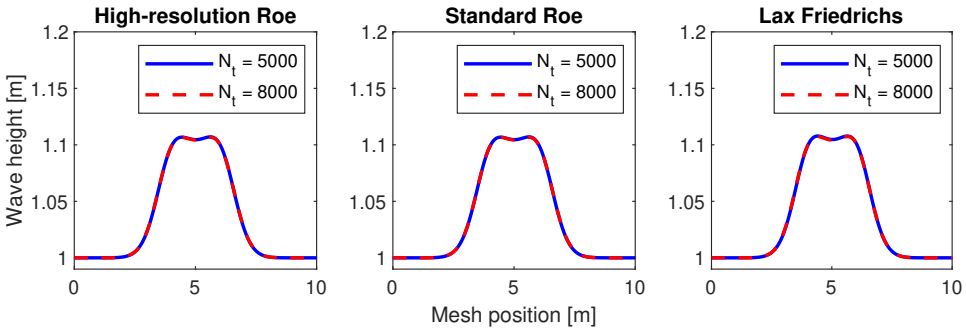

Figure 18: Mesh position at $t = 0.25$ s for different numerical scheme and for different value of N_t

On figure 18, there is not a noticeable difference on the three schemes, the curves are overlapping on each other. At point, we cannot say if the dissipation with the High-resolution Roe scheme is smaller with the other schemes.

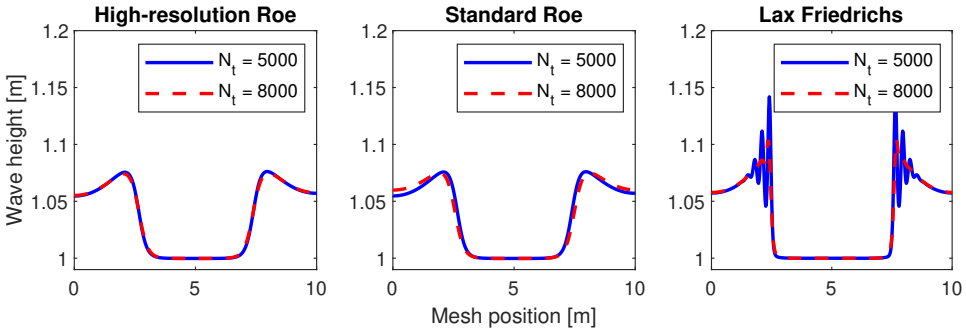

Figure 19: Mesh position at $t = 5$ s for different numerical scheme and for different value of N_t

On figure 19, the difference on the Standard Roe scheme and the Lax Friedrichs scheme are quite noticeable.

On the Standard Roe scheme, the curves are not exactly the same, they are not overlapping on each over. That can maybe be explained by the fact that a different timestep can make the wave goes faster or slower.

On the Lax Friedrichs scheme, the value of N_t has a consequence on the stability of the solution on the top of the wave. It seems that the smaller N_t is, the more oscillations there are at the top of the wave.

As for the High-resolution Roe scheme, such a variation of N_t does not seem to change the form or the stability of the solution. The curves overlap on each over.

We can now say that the High-resolution Roe scheme has smaller dissipation than the other two schemes.

4.1.2 Timestep restriction

The timestep restriction is:

$$c_{max} \frac{\Delta t}{\Delta x} \leq s \tag{11}$$

For this part, we ran the code several times with different value of n in order to find the minimal value of N_t where the code gives a solution that is not complex. At the same time it was looking for c_{max} for each value of n in order to calculate s. We got the following table:

n	minimal N_t	s
100	348	0.0977
200	701	0.0997
300	1054	0.1214
400	1409	0.0882
500	1764	0.0880
600	2119	0.0958
700	2476	0.0914

It seems that the time step restriction defined by the equation 11 is valid, because all the values of s are quite close, except for $n = 300$ but it does not seem to be an issue here, since we are looking for a minimal value of s. So, it seems that there

is constant $s \leq 0.0880$ that exists which can prove that the time step restriction is still defined by equation 11.

4.2 Comparison of the four different types of solution (from section 3.2) with the standard Roe scheme

In this part, we are going to compare the High-resolution Roe scheme with the standard Roe scheme by displaying both graphs for each type, and also by showing the difference Δh and Δu between both scheme.

$$\Delta = \text{High-resolution scheme} - \text{Standard scheme}$$

Every following graph has been plotted with **80 cells**. For each type of solution, we have $\mathbf{\Delta t = 0.01}$ [s] and $\mathbf{\Delta x = 0.125}$ [m]

4.2.1 Type 1 and 2

From what we can see, the differences between both scheme are not apparent for these types of solution. On the right graphs, we can see that they are very slight, but they seem to reach their peak around the middle.

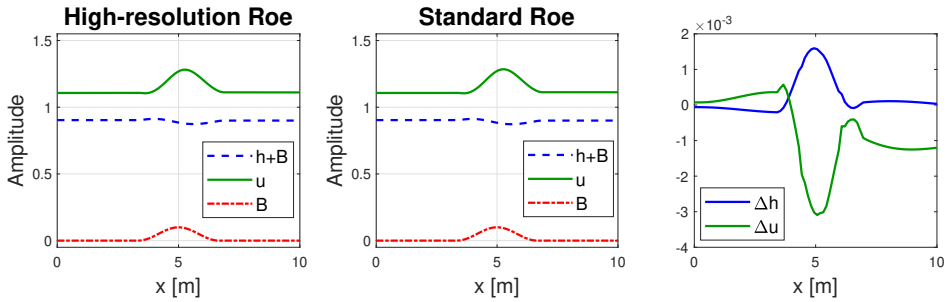

Figure 20: Comparison of type 1 solution between High-resolution and standard Roe scheme. $\mathbf{t = 40s}$

It corresponds for type 1 (fig. 20) at the position where the amplitude is the lowest and also where the velocity is the highest. From the right graph, we can say that the bump is slightly shallower for the High-resolution scheme in comparison to the standard scheme. But it seems that for this type of solution both schemes give similar result.

As for type 2 (fig. 21), it corresponds to the position where the amplitude is the highest and where the velocity is the lowest. In this case the bump is a slight smaller with the High-resolution scheme. Again it seems that both schemes give similar solution for this type.

4.2.2 Type 3 and 4 without entropy fix

For type 3 (fig. 22), there is an apparent difference between both scheme. At $x = 7.722$ [m], a peak can be seen on the right graph, this position coincides with the position where the discontinuity ends. So it seems that for the High-resolution

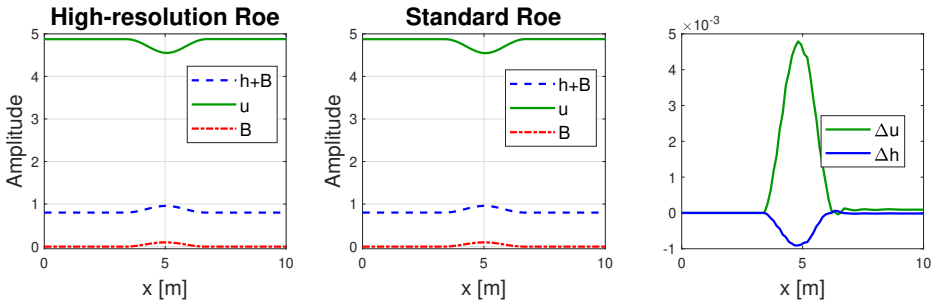

Figure 21: Comparison of type 2 solution between High-resolution and standard Roe scheme. $\mathbf{t = 20s}$

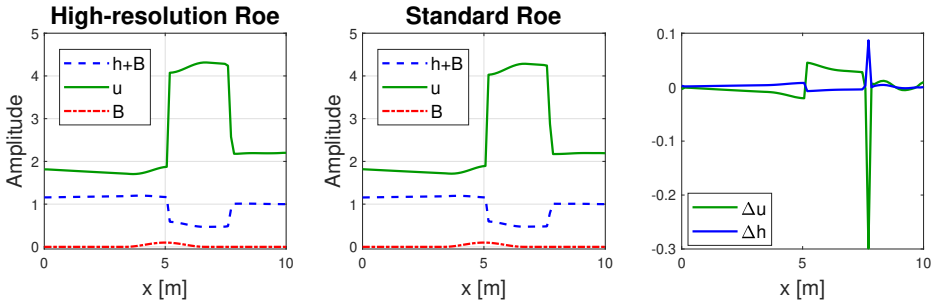

Figure 22: Comparison of type 3 solution between High-resolution and standard Roe scheme. $\mathbf{t = 20s}$

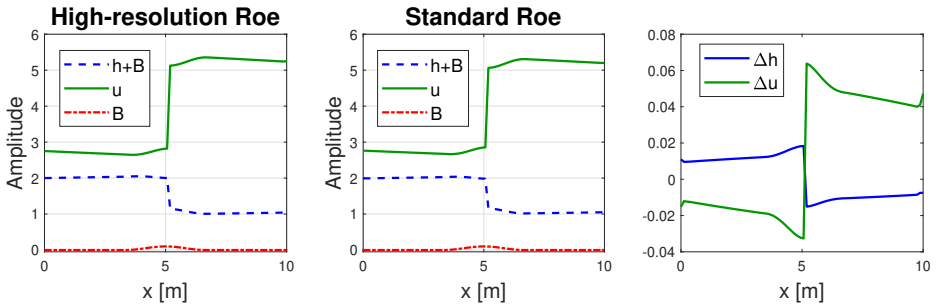

Figure 23: Comparison of type 4 solution between High-resolution and standard Roe scheme. $\mathbf{t = 20s}$

Roe scheme it ends one cell ahead in comparison to the standard scheme. If we ignore the peak, we can see that the difference is quite big, nonetheless, in comparison to the previous types of solution.

As for type 4 (fig. 23), the results seem close, but if we look to the right graph, we can see that the difference between both between both schemes is quite big, rather similar to the previous type.

4.2.3 Type 3 and 4 with entropy fix

In this part, we fix the discontinuities in type 3 and 4 by adding an entropy term into both schemes seen in section 3.2.3.

For type 3 (fig. 24), the peak is still present, but seems to be smaller which

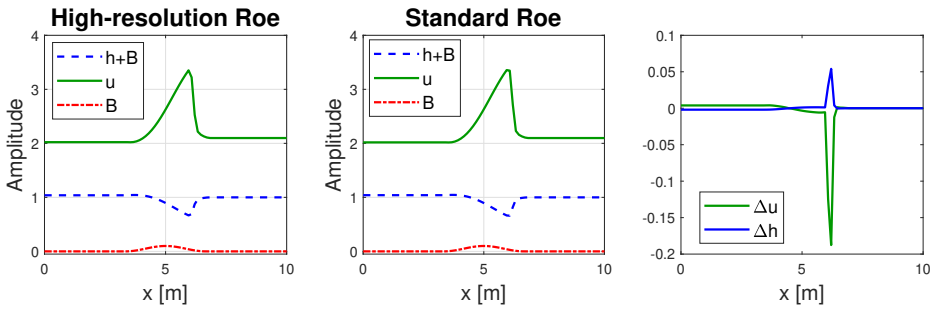

Figure 24: Comparison of type 3 with entropy fix solution between High-resolution and standard Roe scheme. $\mathbf{t = 20s}$

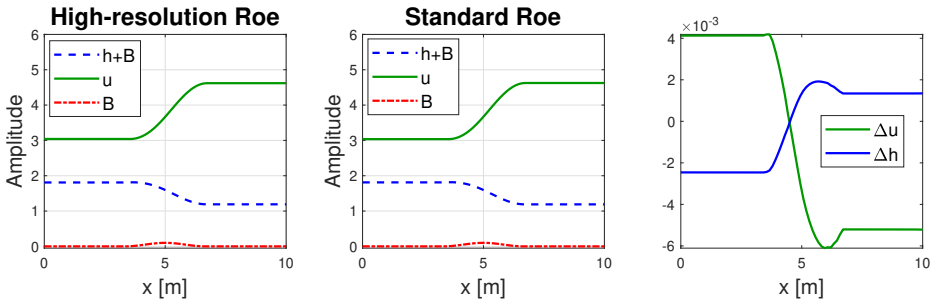

Figure 25: Comparison of type 4 with entropy fix solution between High-resolution and standard Roe scheme. $\mathbf{t = 20s}$

can be explained by the fact that the discontinuity disappears with the entropy fix. Moreover, the difference between both scheme is much smaller compared to the case without entropy fix.

As for type 4 (fig. 25), after fixing the entropy, the difference is also smaller in comparison to figure 23.

5 Conclusion

To conclude on this report, we have been computing the wave equation for an uneven bottom. We have seen what it implied to use the Roe scheme and more generally the Lax-Friedrich scheme as well as a high-resolution Roe scheme.
Comparing these schemes, we saw several ways of modeling and studying a flow an a tube. We moreover saw how to stick to the physical application by working a the schemes' artificial discontinuities and dissipations.

References

[1] Alessandro Valiani and Lorenzo Begnudelli. Divergence form for bed slope source term in shallow water equations. *Journal of Hydraulic Engineering*, 132:652–665, 07 2006.

[2] Wanxie Zhong Zhenhan Yao, M. W. Yuan. *Computational mechanics : Proceedings of the sixth world congress on computational mechanics in conjunction with the second asian-pacific congress on computational mechanics*. Tsinghua University Press Beijing, 09 2004.